Evaluating root cause: The distinct roles of hydrogen and firing in activating light- and elevated temperature-induced degradation

M. A. Jensen,[1,a)] A. Zuschlag,[2] S. Wieghold,[1] D. Skorka,[2] A. E. Morishige,[1] G. Hahn,[2] and T. Buonassisi[1]
[1]*Department of Mechanical Engineering, Massachusetts Institute of Technology, Cambridge, Massachusetts 02139, USA*
[2]*Department of Physics, University of Konstanz, Konstanz 78457, Germany*

(Received 25 May 2018; accepted 31 July 2018; published online 22 August 2018)

The root cause of light- and elevated temperature-induced degradation (LeTID) in multicrystalline silicon *p*-type passivated emitter and rear cell (PERC) devices is still unknown. Microwave-induced remote hydrogen plasma (MIRHP) is employed to vary the concentration of bulk hydrogen and to separate the effects of hydrogen and firing temperature in LeTID-affected wafers. We find that hydrogen is required for degradation to occur, and that samples fired prior to the introduction of hydrogen do not degrade. Importantly, samples with hydrogen that have not been fired do degrade, implying that the firing time-temperature profile does not cause LeTID. Together, these results suggest that the LeTID defect reaction consists of at least two reactants: hydrogen and one or more defects that can be separately modified by high-temperature firing. We assess the leading hypotheses for LeTID in the context of our new understanding of the necessary reactants. *Published by AIP Publishing*. https://doi.org/10.1063/1.5041756

I. INTRODUCTION

Light- and elevated temperature-induced degradation (LeTID) can cause about 10% relative efficiency degradation in multicrystalline silicon (mc-Si) passivated emitter and rear cell (PERC) devices during the first months of operation.[1] In the field, this degradation can take many years to recover, representing a significant loss to the installed system energy yield over time.[2] While mitigation strategies for LeTID have been suggested with varying success, the root cause of LeTID is still unknown.

Several experimental observations suggest that hydrogen plays a role in LeTID. First, the extent of LeTID depends strongly on the firing peak temperature, with LeTID almost completely suppressed for peak firing temperatures below about 675 °C.[3–5] The dielectric layers used for passivation in PERC devices (e.g., aluminum oxide, silicon nitride) can contain high hydrogen concentrations that are released into the bulk during the firing process. Several studies have directly probed the relationships between dielectric passivation layers, firing time-temperature profile, and LeTID.[6,7] Those studies found that only samples fired after dielectric deposition showed LeTID, and samples with dielectric layers that were not fired did not show LeTID. Recently, Vargas *et al*. varied the silicon nitride deposition conditions to conclude that the extent of LeTID depends on both the firing peak temperature and the hydrogen content of the silicon nitride.[8] Based on this experimental evidence, hydrogen-focused hypotheses have gained increasing interest, with suggestions of hydrogen pairing with a deep-level donor.[5,9,10]

In this contribution, we investigate the effect of hydrogen on LeTID behavior. We distinguish between the competing effects of the firing time-temperature profile and hydrogen by employing microwave-induced remote hydrogen plasma (MIRHP),[11] rather than a hydrogen-rich dielectric, to introduce hydrogen. We find that, while the firing time-temperature profile is not required to activate the defect, hydrogen must be present for degradation to occur. These results imply that: (1) hydrogen does play a determining role in LeTID; (2) the LeTID reaction must involve two or more reactants: hydrogen and one or more defects that can be separately modified in the bulk during metallization firing; and (3) metal precipitate dissolution during firing alone cannot explain the observed degradation.

II. MATERIALS AND METHODS

All samples used in this study were selected from adjacent positions within the same industrial *p*-type mc-Si ingot grown by directional solidification and known to be affected by LeTID, with boron doping 1.3 Ω-cm and thickness 180 μm. As outlined in Fig. 1, ten samples were subjected to the following processes: saw damage removal, phosphorous diffusion gettering (PDG, 835 °C, 35 min), and emitter removal. The ten unpassivated samples were divided into two groups: (A) five samples were left unfired, and (B) five samples were fired with no passivation layers. Firing was performed using a belt furnace with a peak sample temperature of 800–850 °C. Due to the small sample size (4 cm × 5 cm) and to prevent contamination, the samples were fired in a "sandwich" configuration between two larger, clean monocrystalline silicon wafers.

Hydrogen was then intentionally introduced to the wafers from groups A and B using MIRHP. Similar to the experimental design of Wilking *et al*., the concentration of hydrogen was varied using different MIRHP process times, from 0 min up to 120 min, at 350–375 °C.[12] The 0 min

a)Author to whom correspondence should be addressed: jensenma@alum.mit.edu

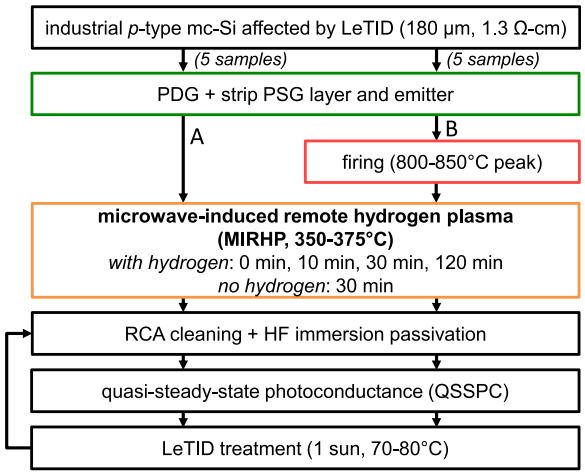

FIG. 1. Process flow for samples analyzed in this experiment. Hydrogen is intentionally introduced to the wafer bulk using the microwave-induced remote hydrogen plasma (MIRHP) process.

treatment time describes a sample that has been subjected only to PDG, emitter removal, and firing (if applicable) prior to degradation and lifetime measurement; such processing conditions are not expected to result in LeTID. To differentiate between the effects of hydrogen and the MIRHP time-temperature profile, one sample from each group was heated at the process temperature for 30 min with no hydrogen plasma.

Direct measurements of the hydrogen concentration after MIRHP are not available for the conditions and materials studied herein. For comparison, Hahn *et al.* measured deuterium (D) concentrations using secondary ion mass spectrometry (SIMS) in ribbon grown on substrate (RGS) silicon solar cells after a MIRHP process using D_2 instead of H_2 gas, 450 °C annealing temperatures, and annealing times ranging from 5 to 24 h.[13] The concentration was the highest near the surfaces, with $[D] \approx 10^{17}\,cm^{-3}$ on the front side and $2 \times 10^{16}\,cm^{-3}$ on the rear side. A symmetric concentration profile was measured with the wafer depth, with the steepest concentration profile measured for the shortest MIRHP time—the authors attributed this distinct concentration profile to trapping at oxygen precipitates. While these results provide a reasonable benchmark for hydrogen concentrations after MIRHP, there are several key differences compared to our experiment that would likely result in different peak [H] and profiles with wafer thickness, including the sample structure during MIRHP, MIRHP process times and temperatures, and substrate parameters.

After processing, the LeTID behavior was probed using quasi-steady state photoconductance (QSSPC) before and after exposure to 1 sun-equivalent illumination (Xenon lamp) at 70–80 °C. To measure the samples with no dielectric layers, surface passivation was accomplished by immersion in hydrofluoric acid (HF) as described in detail by Grant *et al.*[14] The lifetime was measured at several time points along the degradation curve.

Three additional control samples were included in the experiment after processing, including two double-side polished, *p*-type Float-Zone (FZ) samples with doping 2–3 Ω-cm and thickness approximately 275 µm and one mc-Si sample taken from the same sample set as that investigated in Refs. 5 and 15–17. One FZ wafer was degraded with no dielectric layers to check for contamination in the degradation setup (FZ degradation control). The second FZ wafer was left undegraded with no dielectric layers to measure the variation in surface passivation quality during the HF-based lifetime measurement (FZ passivation control). The mc-Si control sample was also used to measure the variation in surface passivation quality (mc-Si passivation control). This sample was selected from a wafer that was fired with a stack of dielectric layers at 750 °C (setpoint, 650 °C estimated sample temperature). The sample, not expected to degrade due to the low firing temperature, was stripped of all dielectric layers and emitter and was left undegraded for the duration of the experiment. All control samples were measured simultaneously with the MIRHP test samples.

III. RESULTS

A. Degradation curves

Figure 2 plots the lifetime at $\Delta n = 6 \times 10^{14}\,cm^{-3}$ and the effective defect density (N_t*) as functions of degradation time for the FZ passivation control (a), Group A unfired samples (b), and Group B fired samples (c). The mc-Si passivation control sample, used to gauge the variation in the mc-Si surface passivation quality and included in Figs. 2(b) and 2(c), was only added to the experiment at 801 610 s. The FZ degradation control, not plotted in Fig. 2, had a stable lifetime measured throughout the experiment, indicating that no external contamination occurred under the degradation conditions. The degradation behavior of a PERC semifabricate sample (not shown) was checked to ensure that the firing sandwich configuration results in LeTID. This semifabricate was fabricated from the same starting wafers, processed through PDG alongside Groups A and B, and coated with aluminum oxide and silicon nitride prior to firing. Firing was performed at the same time and in the same configuration as for Groups A and B. The semifabricate degraded within the measured time, with a distinct change in the injection-dependent lifetime, as expected for LeTID. The maximum effective defect density measured for this PERC semifabricate was $[10.5 \pm 1.0] \times 10^3\,s^{-1}$, slightly lower than that measured for the unfired sample with 10 min MIRHP.

The errors bars are omitted from Fig. 2 for clarity; based on repeated HF-immersion measurements of a stable mc-Si sample with a similar bulk lifetime to the samples studied herein, the expected experimental error for each lifetime data point is approximately ±5%. N_t^* was calculated by the harmonic difference between the estimated Shockley-Read-Hall (SRH) lifetimes. The calculations were done according to the following steps: (1) calculate the injection-dependent surface recombination velocity (SRV) from the FZ passivation control sample according to Ref. 18 and accounting for Auger and radiative recombination;[19] (2) for simplicity, calculate an average and injection-independent SRV from the low-injection data; and (3) calculate the SRH lifetime for the mc-Si samples using the average SRV and accounting for Auger and radiative contributions. We note that, while the actual SRV for the mc-Si wafers may be different from that

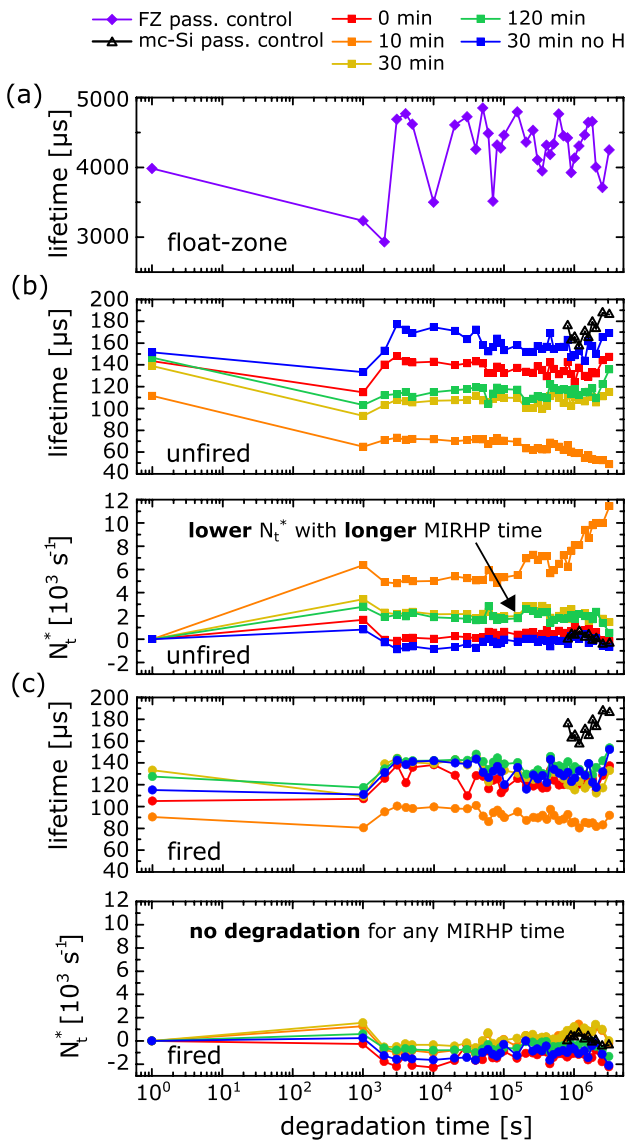

FIG. 2. Degradation behavior for (a) float-zone passivation control, (b) unfired, and (c) fired samples. The same mc-Si passivation control sample is plotted in (b) and (c). For (a)–(c), the lifetime at $\Delta n = 6 \times 10^{14}\,\mathrm{cm}^{-3}$ (top) is plotted versus time exposed to degradation conditions (1 sun-equivalent at 70–80 °C). For (b) and (c), the effective defect density (N_t^*, bottom) is also plotted. N_t^* is calculated using the harmonic difference between the degraded and initial lifetimes after removal of estimated surface and intrinsic recombination mechanisms. The FZ and mc-Si passivation control samples have stable bulk lifetimes and were measured at the same time as all other bare mc-Si wafers using HF immersion.

estimated using the FZ wafers due to both the doping level and surface texture differences, the majority of the measured lifetimes for the mc-Si samples are dominated by SRH recombination due to the low SRV [and correspondingly high FZ passivation control lifetime plotted in Fig. 2(a)] during HF-immersion measurements. As explained in Sec. III B, LeTID is characterized primarily by changes in the bulk lifetime and has been well-characterized using SRH statistics.[5,15,16,20,21] The error for the calculated SRH lifetime is approximately ±15%, assuming independent error propagation, no error associated with the Auger and/or radiative lifetimes, and ±5% error for each measured lifetime. The error for N_t^* depends on the magnitude of the change in lifetime: for large changes in lifetime (e.g., unfired 10 min MIRHP), the error for N_t^* is approximately 45%, while for small changes in lifetime, the error may greatly exceed the value of N_t^*.

The passivation control samples demonstrate consistent and high surface passivation quality [Fig. 2(a) and black triangles in (b) and (c)]. As demonstrated by the FZ passivation control sample in Fig. 2(a), the first several measurements featured the highest variability in the surface passivation quality. Similar variability can be seen in the measured lifetimes for the unfired [Fig. 2(b), top] and fired [Fig. 2(c), top] samples. After exposure to degradation conditions, all unfired samples processed with different MIRHP times and hydrogen degrade in lifetime and correspondingly increase in effective defect density after exposure to LeTID conditions [Fig. 2(b)]. In contrast, the unfired samples with MIRHP and no hydrogen show no or minimal changes in lifetime and effective defect density. Similarly, for the samples fired prior to MIRHP [Fig. 2(c)], no or minimal change is observed in the lifetime and effective defect density for all MIRHP process times (with and without hydrogen) within the measured degradation time (minimum 1000 s intervals up to 3 140 860 s ≈ 872 h).

It is unclear whether regeneration does or will occur for the unfired samples that do degrade. Until the last measurement for the unfired sample with 10 min MIRHP, the lifetime decreases and the sample appears to be in degradation throughout the measured time. For the unfired samples with 30 min and 120 min MIRHP, the lifetime and N_t^* increase and decrease, respectively, toward the end of the measured time. This may indicate the start of regeneration; however, since there is a similar uptick in the measured lifetime for the mc-Si passivation control sample, the increase in lifetime could be explained by a change in the surface passivation quality that is not effectively accounted for with the SRV correction.

It is reasonable to expect that samples without dielectric layers will degrade more slowly than those with dielectric layers. Since the LeTID degradation rate has been found to trend directly with the injection level,[22,23] the degradation rates for the samples measured with HF immersion are expected to be much slower than those for samples with dielectric layers. The H-termination on the surface of the wafer deteriorates quickly after removing the wafer from the HF solution. When the samples are transferred to the degradation setup, the effective wafer lifetimes are limited by surface recombination to several microseconds. Figure S.1 compares the expected difference in degradation behavior for two samples taken from the same wafer, one with and one without dielectric layers in place. The sample without dielectric layers was measured using the HF-immersion passivation method. We note that the maximum effective defect concentration shown in Fig. S.1 is higher than that reported for any sample in Fig. 2. The lower effective defect concentration in the MIRHP samples may be due to differences in the starting wafer quality and/or processing conditions.

B. Injection-dependent lifetime

It is unclear based on the degradation curves alone whether the degradation defect activated in this experiment

is the same as that causing LeTID. To further investigate the defect in our samples, we employed lifetime spectroscopy to probe the change in the injection-dependent lifetime during degradation. Previous studies have shown that this type of analysis can yield important information about the evolving recombination activity of the LeTID defect.[16] The injection-dependent signature of the LeTID defect is the appearance of a defect at the maximum degradation point with an electron-to-hole capture cross-section ratio (k-value) between 26 and 36 at midgap.[15] In previous work, the change in defect recombination was assessed throughout both degradation and regeneration to conclude that LeTID is characterized by a defect that appears early in degradation and primarily changes in concentration (constant k-value) as degradation proceeds.[16] For this H-focused study, the samples that degrade as shown in Fig. 2(b) are expected to be characterized by a change in defect recombination towards a defect with similar k-values to previous LeTID studies if the same defect has been activated. The injection-dependent lifetime analysis presented in this section demonstrates that the defect measured in the unfired samples with 10, 30, and 120 min MIRHP with hydrogen has the same characteristics as that measured previously for wafers affected by LeTID.

To quantitatively assess the change (or lack of change) in injection-dependence, the measured lifetime was fit with two independent defects per the procedure described in Refs. 15 and 24. In this case, the injection-dependent SRH lifetime is evaluated as previously described by assessing the surface lifetime using an estimation of SRV from the FZ passivation control sample. It is important to note that samples measured using HF-immersion passivation are not susceptible to the same degradation in surface passivation quality throughout degradation as those with dielectric layers.[25] The lifetimes and defect parameters calculated for these samples therefore represent variation primarily in bulk rather than surface recombination. The fit parameters for each defect are then translated to defect parameters (k and inverse electron time constant, $1/\tau_{n0}$) as functions of the energy level within the bandgap (see Figs. 3 and 4). For simplicity in evaluation (i.e., rather than plotting the full E_t–k curve), the parameters are calculated at the intrinsic energy and plotted for the unfired samples (10, 30, and 120 min MIRHP) in Fig. 3 and for the fired samples (0 and 10 min MIRHP) in Fig. 4. In some cases, the defect is shallow and the k-value cannot be evaluated at the intrinsic energy. Instead, a marker is placed at the bottom of the plot and is labelled "shallow" at the corresponding location on the y-axis. The filled circles or squares indicate that the respective defect dominates the SRH lifetime at $\Delta n = 6 \times 10^{14}\,\mathrm{cm}^{-3}$. The k-value range for the LeTID defect previously identified by Morishige, Jensen *et al.* is plotted for comparison with two dashed lines in subplots (a) and (c) of Figs. 3 and 4.[15] To verify that the same defect parameters are expected to be measured using the HF-immersion passivation technique, the lifetimes shown in Fig. S.1 were fitted using the same methodology described above. The results are shown in Fig. S.2 and confirm that the expected k-values can be measured with the HF-immersion technique.

The samples that do not degrade [fired 0 min, Figs. 4(a) and 4(b); and fired 10 min, Figs. 4(c) and 4(d)] have constant k and $\tau_{n0}{}^{-1}$ values for both defects during the measured time period. This indicates a minimal change in recombination activity of the defects present in the wafer, resulting in a stable injection dependence. Similar behavior was observed for all samples that do not degrade per Fig. 2 (data not shown: unfired 0 min and 30 min no H and fired 30 min, 120 min, and 30 min no H).

In contrast, samples that do degrade show changes in one or both defects during degradation. For the unfired 10 min MIRHP sample [Figs. 3(a) and 3(b)], defect 1 is consistently a shallow defect with nearly constant $\tau_{n0}{}^{-1}$, while defect 2 quickly increases from a low k-value to a k-value in the expected range for the LeTID defect. As in the previous study of LeTID defect parameters throughout degradation, while the k-value remains nearly constant within the expected range during most of the degradation, $\tau_{n0}{}^{-1}$ increases.[16] $\tau_{n0}{}^{-1}$ is

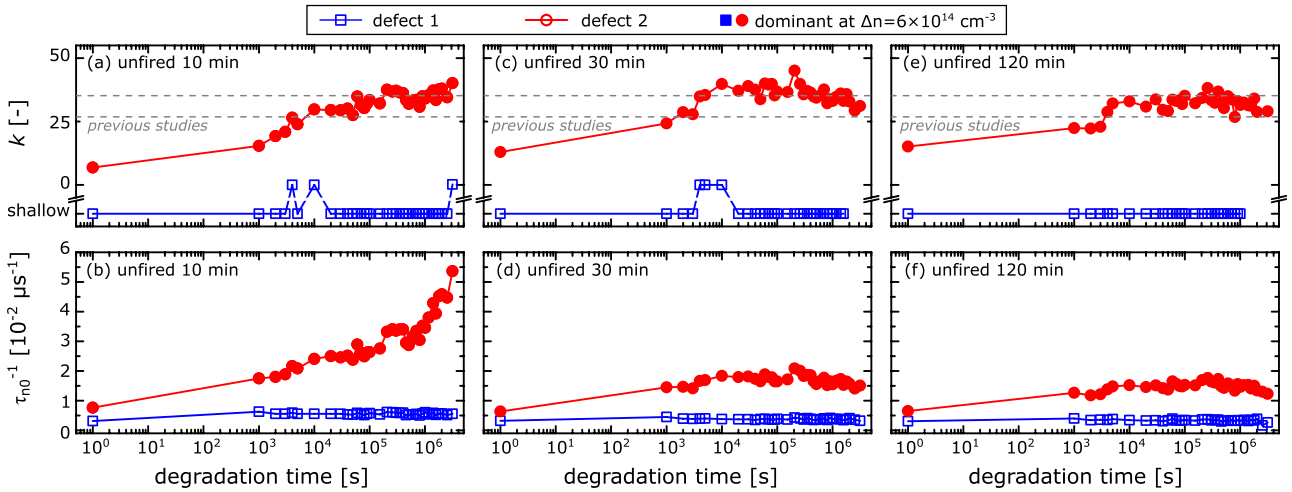

FIG. 3. Ratio of electron-to-hole capture cross-section (k-value) and inverse electron time constant ($\tau_{n0}{}^{-1}$), calculated at the intrinsic energy level, plotted versus degradation time for the following samples: (a) and (b) unfired with 10 min MIRHP, (c) and (d) unfired with 30 min MIRHP, and (e) and (f) unfired with 120 min MIHRP. A two-defect fit is used to fit the linearized Shockley-Read-Hall lifetime at each time. The filled circles/squares indicate that the respective defect dominates the SRH lifetime at $\Delta n = 6 \times 10^{14}\,\mathrm{cm}^{-3}$. The dashed gray lines indicate the LeTID k-value range as identified in Refs. 15 and 16.

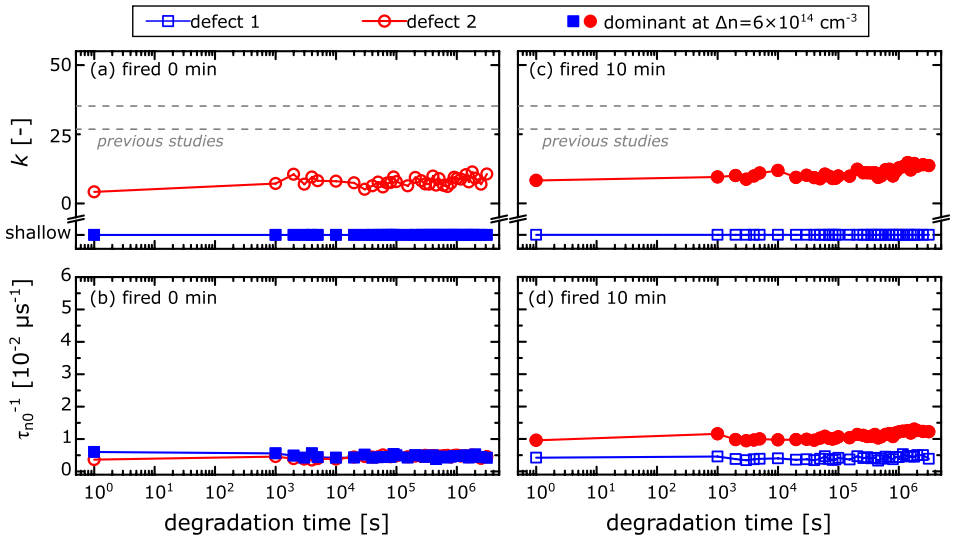

FIG. 4. Same as Fig. 3 for the following samples: (a) and (b) fired with 0 min MIRHP and (c) and (d) fired with 10 min MIRHP.

proportional to the defect concentration; when the k-value of defect 2 is constant, it is likely that the same defect is being measured (constant σ_n and v_{th}), and therefore an increase in τ_{n0}^{-1} indicates an increase in the defect concentration. Similar behavior was observed for the unfired 30 min MIRHP [Figs. 3(c) and 3(d)] and unfired 120 min MIRHP [Figs. 3(e) and 3(f)] samples. The change in τ_{n0}^{-1} is less pronounced for the latter two samples, which would be expected if the LeTID defect concentration is lower in these samples as suggested in Fig. 2(b). Therefore, we conclude that the defect causing degradation in the unfired MIRHP samples is the same as that responsible for LeTID.

IV. DISCUSSION

A. Distinguishing hydrogen from firing

Several insights can be derived about the role of hydrogen in LeTID by analyzing the degradation behavior for this experiment. By comparing the unfired samples with 0 min MIRHP and 30 min MIRHP no H to those with 10, 30, and 120 min MIRHP with H, we conclude that hydrogen is required for degradation to occur in the unfired samples. Further, by directly comparing the results for the samples processed with MIRHP for 30 min with and without hydrogen, we conclude that it is the presence of hydrogen, rather than the time-temperature profile of the MIRHP process (plateau at 350–375 °C), that results in the observed degradation behavior. Previous studies of firing and dielectric layers suggested that firing was required in the presence of a hydrogen-rich dielectric layer.[6,7] In this study, we are able to differentiate between the role of hydrogen and the necessity of the firing time-temperature profile. These results demonstrate that the firing time-temperature profile itself is not required for degradation to occur and that hydrogen introduced by methods other than firing of dielectric layers can cause LeTID. We note that the maximum N_t^* measured for the unfired sample with 10 min MIRHP and the PERC semifabricate are comparable to those measured by Vargas *et al.* for a fired silicon nitride layer with the following parameters: PECVD deposition at 350 °C, pre-firing hydrogen fraction between 12% and 12.5%, firing peak temperature 748°–825°, and 5%–20% hydrogen fraction released during firing.[8]

B. Evidence for two or more reactants leading to LeTID: Firing prior to hydrogenation

For the fired samples, N_t^* remains nearly constant as the degradation time increases [Fig. 2(c)], and the fitted defect parameters do not change during the measured degradation time (Fig. 4). Given this behavior, there are at least two distinct possibilities: (1) both degradation and regeneration occurred within the initial 1000 s time interval, or, more likely, (2) the wafer was altered in some way during firing, prior to the introduction of hydrogen, to prevent LeTID defect formation. In the first case, the high-temperature firing process may have acted as a "pre-anneal," affecting the degradation behavior. To assess this possibility, a second replicate of the same experiment (Fig. S.3) was measured through 113 020 s with more frequent intervals between 0 s and 1000 s. This second replicate demonstrated similar trends with processing conditions as those shown in Figs. 2 and 4, with no apparent fast degradation, regeneration, and/or change in injection dependence before 1000 s for any of the non-degrading samples. Lifetime spectroscopy analysis (as in Figs. 3 and 4) showed that the steady degradation observed for all samples shown in Fig. S.3 is associated with variations in surface passivation quality during the measurements rather than modulation of the LeTID defect.

The second possibility is a more likely explanation for the lack of degradation in the fired samples, as there may have been precipitation, dissolution, out-diffusion, and/or reconfiguration (e.g., pairing in a stable way with a nearby atom or vacancy) of a necessary LeTID reactant during the firing process. Since hydrogen is introduced using MIRHP after the firing process, we hypothesize that the reactant modified by firing is not hydrogen but instead an additional reactant required to cause LeTID. These results provide evidence for an LeTID reaction that consists of at least two reactants: (1) hydrogen and (2) one or more defects that can be modified separately by firing. Similar experiments were performed by Kersten *et al.*[6] and Winter *et al.*[7] in which

PERC semifabricates did not degrade when the sample was fired prior to passivation. The authors of both studies concluded that a hydrogen-rich dielectric layer must be present during firing, which is consistent with the conclusion presented herein. However, it is also possible that the lack of degradation they observe for the samples fired prior to passivation is due to the same effect observed in this study for samples fired prior to MIRHP.

C. Trends with MIRHP processing time

To study the change in N_t^* due to the different MIRHP times, the maximum (in terms of degradation time for each sample) N_t^* is plotted in Fig. 5 versus MIRHP process time for both the unfired and fired samples. The plotted error bars were calculated according to the method described previously. For reference, the minimum and maximum error bounds are plotted as shaded areas for both the unfired and fired samples with 30 min MIRHP time but no H. We note that, while additional MIRHP times between 0 and 30 min should be tested, the unfired 10 min MIRHP sample has the highest N_t^*, after which N_t^* decreases with longer MIRHP process time.

There are two possible explanations for the observed trend with MIRHP process time: (1) longer MIRHP times may correspond to higher hydrogen concentrations, indicating a relationship between bulk hydrogen concentration and suppression of LeTID; or (2) the time-temperature profile of the MIRHP process may be primarily responsible for difference in the degradation extent. According to the first possible explanation, as MIRHP process time increases, the hydrogen concentration in the wafer increases and results in a decreasing N_t^* as the bulk hydrogen content increases above 10 min. Higher hydrogen concentrations could result in formation of molecular hydrogen, reducing the amount of hydrogen available to participate in the LeTID reaction, or the LeTID regeneration reaction could occur very quickly in the presence of higher hydrogen concentrations. Since the hydrogen concentration was not directly measured in this experiment, it is difficult to comment definitively on the relationship between the extent of degradation and hydrogen concentration. Vargas *et al.* recently reported similar results for fired SiN_x layers with increasing hydrogen content, although the possible trend with hydrogen is less clear than the results presented herein.[8]

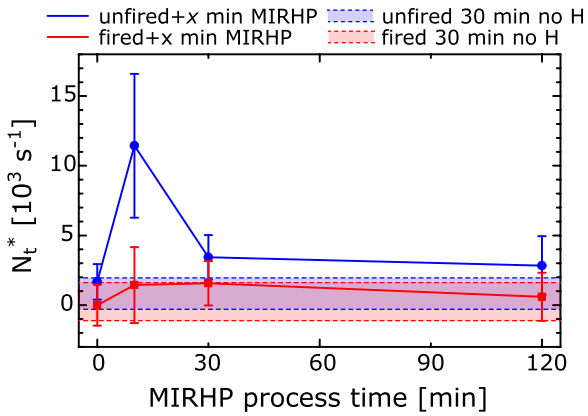

FIG. 5. Maximum effective defect density (N_t^*) measured for the unfired and fired samples as a function of MIRHP process time in minutes. Longer MIRHP process times correspond to higher hydrogen concentrations. For samples where MIRHP time was not varied (unfired and fired 30 min MIRHP time with no H), the minimum and maximum N_t^* bounds are plotted as shaded areas. N_t^* is calculated as previously described, and lifetimes are evaluated at $\Delta n = 6 \times 10^{14}\,\mathrm{cm}^{-3}$.

According to the second possible explanation, the degradation behavior may have been altered by the MIRHP time and temperature, resulting in lower maximum N_t^* during the measured time. Chan *et al.* found slower degradation rates and less degradation after annealing in the dark up to 275 °C.[26] In that work, the most significant changes in performance occurred for anneals longer than 10 min. To test this hypothesis, samples were prepared from the same starting material as that described herein and processed as PERC semifabricates with a fired, symmetric AlO_y/SiN_x passivation stack. After dielectric deposition and firing, samples were annealed in a nitrogen-rich environment at 350 °C for 10 min, 30 min, and 120 min. The lifetime degradation behavior was quantified, shown in Fig. S.4. The N_t^* for these samples shows a similar trend with annealing time as that observed in the unfired MIRHP experiment, indicating that the time-temperature profile may be responsible for these differences rather than a change in the hydrogen concentration. We note that the observed difference may be due to instability of the fired dielectric layer to annealing.[27] It is also possible that annealing at these moderate temperatures results in a change in the hydrogen configuration in the wafer, as has previously been noted especially for anneals at 200 °C and which could occur during either the MIRHP process or the anneal after dielectric firing.[28]

V. IMPLICATIONS FOR LeTID HYPOTHESES

Based on the results presented herein, a simple description of LeTID can be developed. These results clearly indicate that hydrogen is required for LeTID, that the firing time-temperature profile is not required to activate LeTID, and that one or more of the LeTID defect reactants can be modified and/or passivated by high-temperature firing with no hydrogen source to prevent degradation. The latter observation may suggest, for example, a medium-to-fast diffuser for the non-hydrogen component or passivation of a necessary LeTID reactant by a medium-to-fast diffusing element. While the suggestion of a fast diffuser is consistent with other investigations into solubility and diffusivity restrictions on the LeTID defect,[9,10,29] further experiments are required to investigate the nature of the non-hydrogen component.

Two plausible hydrogen-centric hypotheses for how LeTID occurs are as follows: (1) hydrogen-based complexes form just before degradation, and those complexes dissociate during degradation to reveal increasing concentrations of a background defect; or (2) recombination-active hydrogen-based complexes form in increasing concentrations during degradation. To pinpoint candidate hydrogen-based complexes and/or test these and other hypotheses, further research is needed to understand the role of hydrogen in LeTID. In addition to confirming the results presented

herein, one promising axis of investigation is to assess the stability to dark annealing of the LeTID defect in different states (e.g., before degradation, at maximum degradation, after regeneration). For example, experimental results could be compared to deep-level transient spectroscopy (DLTS) investigations of metal-hydrogen complexes to determine candidate complexes for each state (e.g., Refs. 30–37).

VI. CONCLUSION

In this contribution, we present an analysis of degradation behavior after intentionally varying the hydrogen concentration in LeTID-affected *p*-type mc-Si lifetime samples. By employing MIRHP to introduce hydrogen, we are able to differentiate between the effects of hydrogen and the firing time-temperature profile. Importantly, samples that have been fired prior to hydrogenation do not degrade, while those that have not been fired prior to hydrogenation do degrade. We draw two main conclusions from this work: (1) hydrogen is a prerequisite for LeTID and (2) the firing time-temperature profile alone does not cause LeTID to occur. Together, our results imply that the LeTID defect reaction consists of at least two reactants—hydrogen and one or more defects that can be independently modified by a high-temperature firing process. We further note in our results that longer hydrogenation process times lead to lower effective defect density. This observation may be due either to a relationship between the LeTID defect and bulk hydrogen concentration (less likely) or to the time-temperature profile during the hydrogenation process that affects the degradation behavior similar to a dark anneal (more likely). Based on these results, we summarize the implications of our findings on further research into LeTID. These results are a crucial piece toward identifying the root-cause and solving the "puzzle" of LeTID.

SUPPLEMENTARY MATERIAL

See supplementary material for a comparison of degradation behavior with and without dielectric layers, an additional replicate of the experiment described herein, and an investigation of degradation behavior after dark annealing.

ACKNOWLEDGMENTS

This work was supported by the National Science Foundation (NSF) and the Department of Energy (DOE) under Grant No. NSF CA EEC-1041895. The work of M. A. Jensen was supported by the National Science Foundation Graduate Research Fellowship under Grant No. 1122374. Part of this work was funded by the German BMWi under Contract Nos. 0324001 and 0324204B. The authors would like to thank J. Hofstetter, H. Hieslmair, N. Grant, and Z. Hameiri for the useful feedback and correspondence, and T. Felisca and M. Castillo for assistance with HF-immersion measurements.

[1]K. Ramspeck *et al.*, "Light induced degradation of rear passivated mc-Si solar cells," in *Proceedings of the 27th European Photovoltaic Solar Energy Conference* (2012), pp. 861–865.

[2]F. Kersten *et al.*, "Degradation of multicrystalline silicon solar cells and modules after illumination at elevated temperature," Sol. Energy Mater. Sol. Cells **142**, 83–86 (2015).

[3]C. E. Chan *et al.*, "Rapid stabilization of high-performance multicrystalline p-type silicon PERC cells," IEEE J. Photovoltaics **6**(6), 1473–1479 (2016).

[4]D. Bredemeier, D. Walter, S. Herlufsen, and J. Schmidt, "Lifetime degradation and regeneration in multicrystalline silicon under illumination at elevated temperature," AIP Adv. **6**(3), 35119 (2016).

[5]K. Nakayashiki *et al.*, "Engineering solutions and root-cause analysis for light-induced degradation in p-type multicrystalline silicon PERC modules," IEEE J. Photovoltaics **6**(4), 860–868 (2016).

[6]F. Kersten, J. Heitmann, and J. Muller, "Influence of Al2O3 and SiNx passivation layers on LeTID," Energy Procedia **92**, 828–832 (2016).

[7]C. Winter, A. Zuschlag, D. Skorka, and G. Hahn, "Influence of dielectric layers and thermal load on LeTID," AIP Conf. Proc. **1999**, 130020 (2018).

[8]C. Vargas *et al.*, "Carrier-induced degradation in multicrystalline silicon: Dependence on the silicon nitride passivation layer and hydrogen released during firing," IEEE J. Photovoltaics **8**(2), 413–420 (2018).

[9]D. Bredemeier, D. C. Walter, and J. Schmidt, "Possible candidates for impurities in mc-Si wafers responsible for light-induced lifetime degradation and regeneration," Sol. RRL **2**, 1700159 (2018).

[10]T. Niewelt, F. Schindler, W. Kwapil, R. Eberle, J. Schön, and M. C. Schubert, "Understanding the light-induced degradation at elevated temperatures: Similarities between multicrystalline and floatzone p-type silicon," Prog. Photovoltaics **26**(8), 533–542 (2017).

[11]M. Spiegel, S. Keller, P. Fath, G. Villeke, and E. Bucher, "Microwave induced remote hydrogen plasma (MIRHP) passivation of solar cells using different silicon base materials," *Proceedings of the 14th EU-PVSEC* (1997), pp. 743–746.

[12]S. Wilking, A. Herguth, G. Hahn, S. Wilking, A. Herguth, and G. Hahn, "Influence of hydrogen on the regeneration of boron-oxygen related defects in crystalline silicon Influence of hydrogen on the regeneration of boron-oxygen related defects in crystalline silicon," J. Appl. Phys. **113**, 194503 (2013).

[13]G. Hahn *et al.*, "Hydrogenation of multicrystalline silicon—the story continues," in Proceedings of the 19th EU-PVSEC (2004).

[14]N. E. Grant, "Light enhanced hydrofluoric acid passivation: A sensitive technique for detecting bulk silicon defects," J. Visualized Exp. **107**, e53614 (2016).

[15]A. E. Morishige *et al.*, "Lifetime spectroscopy investigation of light-induced degradation in p-type multicrystalline silicon PERC," IEEE J. Photovoltaics **6**(6), 1466–1472 (2016).

[16]M. A. Jensen, A. E. Morishige, J. Hofstetter, D. B. Needleman, and T. Buonassisi, "Evolution of LeTID defects in p-type multicrystalline silicon during degradation and regeneration," IEEE J. Photovoltaics **7**(4), 980–987 (2017).

[17]M. A. Jensen *et al.*, "Assessing the defect responsible for LeTID: Temperature- and injection- dependent lifetime spectroscopy," in Proceedings of the 44th IEEE Photovoltaic Specialists Conference (2017).

[18]A. B. Sproul, "Dimensionless solution of the equation describing the effect of surface recombination on carrier decay in semiconductors," J. Appl. Phys. **76**(5), 2851–2854 (1994).

[19]A. Richter, S. W. Glunz, F. Werner, J. Schmidt, and A. Cuevas, "Improved quantitative description of Auger recombination in crystalline silicon," Phys. Rev. B: Condens. Matter Mater. Phys. **86**(16), 165202 (2012).

[20]D. Bredemeier, D. Walter, S. Herlufsen, and J. Schmidt, "Understanding the light-induced lifetime degradation and regeneration in multicrystalline silicon," Energy Procedia **92**, 773–778 (2016).

[21]C. Vargas *et al.*, "Recombination parameters of lifetime-limiting carrier-induced defects in multicrystalline silicon for solar cells," Appl. Phys. Lett. **110**(9), 92106 (2017).

[22]W. Kwapil, T. Niewelt, and M. C. Schubert, "Kinetics of carrier-induced degradation at elevated temperature in multicrystalline silicon solar cells," Sol. Energy Mater. Sol. Cells **173**, 80–84 (2017).

[23]D. Bredemeier, D. Walter, and J. Schmidt, "Light-induced lifetime degradation in high-performance multicrystalline silicon: Detailed kinetics of the defect activation," Sol. Energy Mater. Sol. Cells **173**, 2–5 (2017).

[24]J. D. Murphy *et al.*, "Parameterisation of injection-dependent lifetime measurements in semiconductors in terms of Shockley-Read-Hall statistics: An application to oxide precipitates in silicon," J. Appl. Phys. **111**, 113709 (2012).

[25]D. Sperber, A. Graf, D. Skorka, A. Herguth, and G. Hahn, "Degradation of surface passivation on crystalline silicon and its impact on light-induced degradation experiments," IEEE J. Photovoltaics **7**(6), 1627–1634 (2017).
[26]C. Chan *et al*., "Modulation of carrier-induced defect kinetics in multicrystalline silicon PERC cells through dark annealing," Sol. RRL **1**(2), 1600028 (2017).
[27]D. Sperber, A. Heilemann, A. Herguth, and G. Hahn, "Temperature and light-induced changes in bulk and passivation quality of boron-doped float-zone silicon coated with SiN x: H," IEEE J. Photovoltaics **7**(2), 463–470 (2017).
[28]S. A. McQuaid, M. J. Binns, R. C. Newman, E. C. Lightowlers, and J. B. Clegg, "Solubility of hydrogen in silicon at 1300 °C," Appl. Phys. Lett. **62**(14), 1612–1614 (1993).
[29]M. A. Jensen *et al*., "Solubility and diffusivity: Important metrics in the search for the root cause of LeTID," IEEE J. Photovoltaics **8**(2), 448–455 (2018).
[30]W. Jost, J. Weber, and H. Lemke, "Hydrogen—cobalt complexes in p-type silicon," Semicond. Sci. Technol. **11**, 525–530 (1996).
[31]S. Leonard, V. P. Markevich, A. R. Peaker, and B. Hamilton, "Passivation of titanium by hydrogen in silicon," Appl. Phys. Lett. **103**(13), 132103 (2013).
[32]J.-U. Sachse, E. Ö. Sveinbjörnsson, W. Jost, J. Weber, and H. Lemke, "Electrical properties of platinum-hydrogen complexes in silicon," Phys. Rev. B **55**(24), 16176–16185 (1997).
[33]J.-U. Sachse, J. Weber, and E. Ö. Sveinbjörnsson, "Hydrogen-atom number in platinum-hydrogen complexes in silicon," Phys. Rev. B **60**(3), 1474 (1999).
[34]J. Sachse and J. Weber, "Deep-level transient spectroscopy of Pd-H complexes in silicon," Phys. Rev. B **61**(3), 1924–1934 (2000).
[35]N. Yarykin, J.-U. Sachse, H. Lemke, and J. Weber, "Silver-hydrogen interactions in crystalline silicon," Phys. Rev. B **59**(8), 5551–5560 (1999).
[36]M. Shiraishi, J. Sachse, H. Lemke, and J. Weber, "DLTS analysis of nickel—hydrogen complex defects in silicon," Mater. Sci. Eng. B **58**, 130–133 (1999).
[37]E. Ö. Sveinbjörnsson and O. Engström, "Reaction kinetics of hydrogen-gold complexes in silicon," Phys. Rev. B **52**(7), 4884 (1995).